New Phytologist

Leaf anatomy mediates coordination of leaf hydraulic conductance and mesophyll conductance to CO_2 in *Oryza*

Dongliang Xiong[1,2], Jaume Flexas[2], Tingting Yu[1], Shaobing Peng[1] and Jianliang Huang[1]

[1]National Key Laboratory of Crop Genetic Improvement, MOA Key Laboratory of Crop Ecophysiology and Farming System in the Middle Reaches of the Yangtze River, College of Plant Science and Technology, Huazhong Agricultural University, Wuhan, Hubei 430070, China; [2]Research Group in Plant Biology under Mediterranean Conditions, Universitat de les Illes Balears, Carretera de Valldemossa Km 7.5, Palma de Mallorca 07122, Illes Balears, Spain

Authors for correspondence:
Dongliang Xiong
Tel: +34 688564278
Email: dlxiong@outlook.com

Jianliang Huang
Tel: +86 27 87284131
Email: jhuang@mail.hzau.edu.cn

Received: *25 April 2016*
Accepted: *5 August 2016*

New Phytologist (2017) **213:** 572–583
doi: 10.1111/nph.14186

Key words: leaf hydraulic conductance (K_{leaf}), leaf vein density, mesophyll conductance (g_m), mesophyll structure, rice (*Oryza*), stomata.

Summary

- Leaf hydraulic conductance (K_{leaf}) and mesophyll conductance (g_m) both represent major constraints to photosynthetic rate (A), and previous studies have suggested that K_{leaf} and g_m is correlated in leaves. However, there is scarce empirical information about their correlation.
- In this study, K_{leaf}, leaf hydraulic conductance inside xylem (K_x), leaf hydraulic conductance outside xylem (K_{ox}), A, stomatal conductance (g_s), g_m, and anatomical and structural leaf traits in 11 *Oryza* genotypes were investigated to elucidate the correlation of H_2O and CO_2 diffusion inside leaves.
- All of the leaf functional and anatomical traits varied significantly among genotypes. K_{leaf} was not correlated with the maximum theoretical stomatal conductance calculated from stomatal dimensions (g_{smax}), and neither g_s nor g_{smax} were correlated with K_x. Moreover, K_{ox} was linearly correlated with g_m and both were closely related to mesophyll structural traits.
- These results suggest that K_{leaf} and g_m are related to leaf anatomical and structural features, which may explain the mechanism for correlation between g_m and K_{leaf}.

Introduction

In order to keep stomata open for capturing CO_2 during photosynthesis, leaves need a continuous water flow through the leaf hydraulic system to replace the water lost by transpiration (Sack & Holbrook, 2006). By measuring leaf hydraulic conductance (K_{leaf}, mmol m^{-2} s^{-1} MPa^{-1}), it is possible to know the efficiency of water transportation through the leaf. However, still little is known about the water transport pathways inside leaves, and particularly outside the xylem (Cochard *et al.*, 2004; Buckley, 2015; Sack *et al.*, 2015). In higher plants, water from the stem enters the petiole and moves through xylem in different vein orders, then exits into the bundle sheath and moves through mesophyll tissue before evaporating into the intercellular airspace and diffusing though stomata. Therefore, K_{leaf} consists of at least two components: inside and outside xylem (K_x and K_{ox}, respectively; mmol m^{-2} s^{-1} MPa^{-1}), and hence, K_{leaf} would be limited by both leaf vein density and distribution as well as outside xylem compartment traits (Sack & Holbrook, 2006; Buckley *et al.*, 2015).

A number of studies have dealt with the partitioning of hydraulic resistance within leaves across a broad range of species, and a large variability has been observed. Sack *et al.* (2005) and Scoffoni & Sack (2015) found that 8–77% of whole leaf hydraulic resistance was situated within the xylem in dicotyledonous species. Other studies reported that leaf hydraulic resistance inside xylem was of minor importance compared with outside xylem (Salleo *et al.*, 2003; North *et al.*, 2013). Further resolution of this question is complicated by the difficulty in measuring K_x or K_{ox} directly, and particularly in a way that gives comparable results for the wide range of types of leaf vein systems that occur in higher plants (Cochard *et al.*, 2004; Nardini *et al.*, 2005, 2010; Sack *et al.*, 2012; North *et al.*, 2013; Sack & Scoffoni, 2013).

Leaf vein systems, as distinct water transport systems, vary greatly from species to species in their arrangement, density, vascular bundle features and xylem conduits within the bundles (Ueno *et al.*, 2006; Blonder *et al.*, 2011; Sack *et al.*, 2012; Sack & Scoffoni, 2013). An empirical correlation of K_{leaf} and venation density, expressed as vein length per area (VLA, mm mm^{-2}) was suggested in early studies. VLA is predicted to correlate positively with K_{leaf} by providing more parallel flow paths through the vein system per leaf area, which increases K_x, and by decreasing flow path length from veins to evaporation sites, which increases K_{ox} (Sack & Frole, 2006; Brodribb *et al.*, 2007; Sack *et al.*, 2013; Buckley *et al.*, 2015). Although studies over the past two decades have found positive, negative or even no correlations between K_{leaf} and VLA (Nardini *et al.*, 2012, 2014; Sack & Scoffoni, 2012; Flexas *et al.*, 2013b; Xiong *et al.*, 2015d), the majority of data show positive

correlations, particularly for minor vein length per unit area (Sack *et al.*, 2015). The correlation between K_{leaf} and VLA might be affected not only by leaf vein features, but also by aspects of anatomy outside of the xylem, such as size and hydraulic permeability of bundle sheath cells, mesophyll thickness and cell wall thickness (Buckley *et al.*, 2015). Features of outside-xylem anatomy that are not directly related to VLA may also be important in determining K_{leaf}, especially through effects on the partitioning of transport among apoplastic, transmembrane and vapor phase pathways (Sheriff & Meidner, 1974; Buckley, 2015; Scoffoni, 2015). Recent model approaches have suggested that water transport in leaves occurs mainly within the liquid phase, but for leaves with low tissue density, significant water transport may also happen in the vapor phase, especially under high irradiance and high temperature conditions (Rockwell *et al.*, 2014; Buckley, 2015). More recently, modeling by Buckley *et al.* (2015) predicted that the contribution of vapor transport to K_{ox} increased from 16% to 65% on average across 14 dicot species when the temperature gradient inside leaves rose from 0 to 0.2°C.

Many attempts have been made to reveal the correlation between K_{leaf} and physiological variables related to photosynthesis. For instance, relationships between K_{leaf} and photosynthetic rate (A), and K_{leaf} and stomatal conductance (g_s) were often observed (Brodribb *et al.*, 2007; Xiong *et al.*, 2015d). In C_3 plants, it has been demonstrated that under current atmospheric conditions A often is strongly limited by CO_2 diffusion conductance, which comprises g_s and mesophyll conductance (g_m) (Flexas *et al.*, 2008, 2012; Evans *et al.*, 2009). The g_s is determined by both stomatal features (size and density) and opening status, and the opening status might be related to K_{leaf} (Brodribb & Holbrook, 2004; Brodribb & McAdam, 2011; Guyot *et al.*, 2012; Ocheltree *et al.*, 2012; McAdam & Brodribb, 2013). Many studies have investigated the effects of leaf anatomical features on g_m. The mesophyll cell wall thickness, mesophyll cell surface area exposed to intercellular air space per leaf area (S_m) and mesophyll cell surface area occupied by chloroplasts exposed to intercellular air space per leaf area (S_c) were suggested to be the key traits limiting g_m (Evans *et al.*, 2009; Tomás *et al.*, 2013; Xiong *et al.*, 2015b). However, although very few studies have investigated the correlation of K_{leaf} and g_m empirically, a positive correlation was found across species (Flexas *et al.*, 2013b) and *Oryza* genotypes (Xiong *et al.*, 2015d). This correlation was hypothesized to result from a common pathway for water and CO_2 inside the mesophyll and/or a role of aquaporins in both water and CO_2 transport (Flexas *et al.*, 2013b). The possibility that vapor phase transport can contribute substantially to measured K_{leaf} suggests that the transport properties of leaf intercellular air spaces may also contribute to coordination between g_m and K_{leaf}. To our knowledge, there have been no previous studies of the correlation of K_{leaf} and g_m in which leaf anatomy was analyzed in parallel.

Wild rice (genus *Oryza*) is an important germplasm resource and is being utilized to improve rice production. Despite sharing a recent common ancestor, *Oryza* species are ecologically and phenotypically diverse. Thus, revealing the coordination of leaf functional, structural and biochemical traits across the *Oryza* genus will help crop breeders to develop new varieties for sustainable agriculture. Giuliani *et al.* (2013) investigated the diversity of leaf structure and how it relates to photosynthesis and transpiration by using 24 rice and wild relatives. Their results highlight that significant correlations occur among structural and functional traits associated with photosynthesis and transpiration. Here, we investigated the impacts of leaf anatomical traits on K_{leaf} and CO_2 diffusion across 11 *Oryza* genotypes to reveal the intrinsic mechanism of correlation between leaf functional and structural traits. The objectives of this study were: to identify the most limiting fraction of K_{leaf} in rice and rice relatives by partitioning it into K_x and K_{ox}; to investigate the impact of variation in leaf anatomical traits on K_{leaf}, g_s and g_m in rice and rice relatives; and to clarify the role of leaf anatomy in coordination of K_{leaf} and g_m.

Materials and Methods

Plant materials

This study was conducted simultaneously with a study of the importance of leaf morpho-anatomical traits in determining leaf hydraulic conductance (K_{leaf}) in rice (Xiong *et al.*, 2015d), and we note that the gas exchange and K_{leaf} values were taken from the previous one, and the data of new parameters that estimated in the current study were collected from the same plants. Eleven genotypes across five *Oryza* genus were used (Table 1). Plants were grown outdoors in 15-l pots (with 13 kg soil) with a density of three plants per pot. Nitrogen (N), phosphorus (P) and potassium (K) were applied as basal fertilizers at a rate of 3.0 g, 1.95 g and 1.95 g per pot, respectively. During the growth period, plants were well watered (at least 2 cm water level was kept) and pests were controlled using chemical pesticides. Measurements were taken on plants between 50 and 70 d after planting.

Gas exchange

Gas exchange measurements were performed between 09:30 h and 15:30 h on nonsenescent fully expanded leaves using an LI-6400XT portable photosynthesis system equipped with a 6400-40 leaf chamber (Li-Cor Inc., Lincoln, NE, USA), in an environmental controlled room (air temperature of 27.8 ± 2.1°C, the photosynthetic photon flux density (PPFD) at leaf surface of 1200 ± 47 μmol m^{-2} s^{-1}, and relative humidity of 77.4 ± 5.3%). Inside the leaf cuvette, leaf temperature was maintained at 28°C, PPFD at 1500 μmol m^{-2} s^{-1} and, leaf-to-air vapor pressure deficit at 1.1–1.4 kPa, and CO_2 concentration was adjusted to 400 μmol mol^{-1} with a CO_2 mixture. After equilibration to a steady state, gas exchange parameters, steady-state fluorescence (F_s) and maximum fluorescence (F'_m) were recorded. Φ_{PSII} was calculated as follows:

$$\Phi_{PSII} = \frac{(F'_m - F_s)}{F'_m}$$

Potential electron transport rate (J) was computed as follows:

$$J = \Phi_{PSII} \cdot PPFD \cdot \alpha\beta$$

(α, leaf absorptance; β, partitioning of absorbed quanta between photosystems II and I). The product αβ was determined,

Table 1 Mean values ± SD of photosynthesis, leaf hydraulic conductance and CO_2 diffusion conductance ($n = 3$–9 plants)

Genotype	Species	A (μmol m^{-2} s^{-1})	K_{leaf} (mmol m^{-2} s^{-1} MPa^{-1})	K_x (mmol m^{-2} s^{-1} MPa^{-1})	$K_{x\text{-Model}}$ (mmol m^{-2} s^{-1} MPa^{-1})	K_{ox} (mmol m^{-2} s^{-1} MPa^{-1})	$K_{ox\text{-Model}}$ (mmol m^{-2} s^{-1} MPa^{-1})	g_s (mol m^{-2} s^{-1})	g_{smax} (mol m^{-2} s^{-1})	g_m (mol m^{-2} s^{-1})
Shanyou 63	*Oryza sativa* L.	22.6 ± 3.1	7.20 ± 0.29	14.3 ± 0.8	15.3 ± 2.7	14.6 ± 1.5	8.6 ± 0.4	0.28 ± 0.02	1.01 ± 0.06	0.30 ± 0.01
Huanghuazhan	*Oryza sativa* L.	31.8 ± 1.9	8.74 ± 0.73	17.0 ± 1.5	21.2 ± 5.1	18.1 ± 2.3	10.5 ± 0.9	0.33 ± 0.03	1.00 ± 0.08	0.25 ± 0.03
N22	*Oryza sativa* L.	20.9 ± 0.4	7.30 ± 0.59	18.3 ± 2.9	22.6 ± 4.3	12.2 ± 0.4	8.4 ± 0.6	0.31 ± 0.01	0.83 ± 0.01	0.21 ± 0.07
Nipponbare	*Oryza sativa* L.	23.9 ± 1.2	7.17 ± 1.19	13.8 ± 2.1	13.3 ± 4.2	15.2 ± 3.2	8.6 ± 1.5	0.28 ± 0.04	1.07 ± 0.04	0.25 ± 0.06
Lat	*Oryza latifolia* L.	35.9 ± 0.9	12.2 ± 0.40	–	29.2 ± 4.7	–	15.2 ± 3.4	0.58 ± 0.07	1.01 ± 0.05	0.47 ± 0.07
Aus	*Oryza australiansis* L.	23.1 ± 0.7	4.93 ± 0.89	14.2 ± 1.7	17.8 ± 4.6	7.7 ± 2.0	5.6 ± 1.1	0.27 ± 0.02	0.92 ± 0.03	0.23 ± 0.04
I90	*Oryza rufipogon* L.	34.8 ± 2.2	5.76 ± 0.21	16.5 ± 0.5	15.2 ± 4.0	14.9 ± 2.3	7.2 ± 0.4	0.48 ± 0.06	1.01 ± 0.08	0.27 ± 0.04
I08	*Oryza punctata* L.	20.5 ± 0.8	3.63 ± 0.55	15.7 ± 5.4	18.2 ± 3.6	5.0 ± 1.3	4.0 ± 0.7	0.23 ± 0.02	1.05 ± 0.08	0.15 ± 0.02
Wcr	*Oryza granulata* L.	17.6 ± 1.1	4.30 ± 0.94	24.0 ± 2.8	27.6 ± 3.1	5.3 ± 1.4	4.6 ± 1.1	0.21 ± 0.03	1.02 ± 0.02	0.10 ± 0.02
Ruf	*Oryza rufipogon* L.	25.2 ± 2.4	4.09 ± 0.31	16.0 ± 2.1	14.6 ± 3.9	5.5 ± 0.7	4.5 ± 0.4	0.32 ± 0.09	0.88 ± 0.05	0.17 ± 0.01
Rhi	*Oryza rufipogon* L.	23.6 ± 2.2	3.31 ± 0.23	–	16.2 ± 2.8	–	4.2 ± 0.6	0.19 ± 0.02	0.98 ± 0.07	0.28 ± 0.08
ANOVA										
Average		24.5 ± 5.5	6.24 ± 2.65	16.6 ± 3.1	19.2 ± 5.4	10.9 ± 5.1	7.4 ± 3.4	0.32 ± 0.12	0.98 ± 0.07	0.24 ± 0.10
Genotype		***	***	**	***	***	***	**	*	***

K_{leaf}, leaf hydraulic conductance; A, leaf photosynthesis; K_x, hydraulic conductance inside xylem; $K_{x\text{-Model}}$, modeled / hydraulic conductance inside xylem; K_{ox}, hydraulic conductance outside xylem; $K_{ox\text{-Model}}$, modeled / hydraulic conductance outside xylem; g_s, stomatal conductance to CO_2; g_{smax}, maximum theoretical stomatal conductance to CO_2; g_m, mesophyll conductance to CO_2.
*, $P < 0.05$; **, $P < 0.01$; ***, $P < 0.001$.

following Valentini *et al.* (1995), from the relationship between $1/4\Phi_{PSII}$ and Φ_{CO2} obtained by varying either light intensity under nonphotorespiration conditions ($O_2 < 1\%$). To do this, light response curves were determined (Xiong *et al.*, 2015d).

The variable J method described in Harley *et al.* (1992) was used to calculate mesophyll conductance of CO_2 (g_m) and CO_2 concentration in chloroplast (C_c). C_c was calculated as follows:

$$C_c = \frac{\Gamma^*(J + 8(A + R_d))}{J - 4(A + R_d)}$$

(Γ^*, CO_2 compensation point in the absence of respiration). Γ^* is related to the Rubisco specific factor, which is conservative for a species but strongly affected by temperature (Bernacchi *et al.*, 2002; Warren & Dreyer, 2006). In the present study, Γ^* value of 40 μmol mol^{-1} typical for *Oryza* plants were assumed following Xiong *et al.* (2015d). R_d is daytime respiration rate, and it was calculated as the intercept of the linear regression of photosynthetic rate (A) on $PPFD \cdot \Phi_{PSII}/4$ using the data from light response curve (Yin *et al.*, 2009). Then, g_m was calculated as follows:

$$g_m = \frac{A}{C_i - C_c}$$

(C_i, intercellular CO_2 concentration). For all the selected genotypes, g_m was also estimated by using the $A - C_i$ curve-fitting method (Ethier & Livingston, 2004), and a tight correlation was obtained between the two estimates of g_m considering all the data averaged per genotype ($R^2 = 0.99$, $P < 0.001$; Fig. S1b in Xiong *et al.*, 2015d). As the g_m values from both methods were very similar, we used the values obtained by the variable J method to compare with other parameters.

Leaf hydraulic conductance

Measurements were made on nonsenescing and fully expanded leaves of two adjacent tillers on each plant (one for K_{leaf} and another for leaf hydraulic conductance inside xylem (K_x)) and nine plants for each genotype were used. The tillers were harvested under water and kept submerged until measurements were performed. K_{leaf} was measured using the evaporative flux method (EFM) (Sack *et al.*, 2002; Brodribb *et al.*, 2007; Sack & Scoffoni, 2012; Xiong *et al.*, 2015d). Leaves were excised under the water and placed under conditions favorable to transpiration (i.e. under PPFD of 1200 μmol m^{-2} s^{-1} and air temperature of 28°C). In order to ensure a tight seal with tubing that supplied water, first, leaf sheaths' vertical coating surrounding the cone-shaped plastic stick (the gap between leaf sheath and stick was sealed up by using petroleum jelly and adjusting the position of the stick), and then the outside of sheathes were wrapped in thread seal tape (polytetrafluoroethylene film). The tubing system was connected to a plastic erlenmeyer flask (250 ml) with degassed water situated on analytical balance (Sartorius BP 2215, Göttingen, Germany). Before measuring, the leaks were checked by creating a high gradient (*c.* 60 cm) between leaves and water surface in the

erlenmeyer flask. When leaves reached steady state (the water weight lost linearly with time, typically, *c.* 20 min), the weight of water was recorded every 60 s and the water flow rate was calculated as the slope of linear regression between weight and time (15 min). The leaf area was measured using a portable leaf area meter (LI-Cor 3000C; Li-Cor Inc.) and then the liquid water flow rate was normalized by leaf area (E). The leaves were detached and cut into small sections and mixed immediately (< 20 s), and the subsamples were used for leaf water potential (Ψ_{leaf}) measuring by using a WP4C Dew point Potential Meter (Decagon, Pullman, WA, USA). K_{leaf} was calculated as follows:

$$K_{leaf} = \frac{E}{\Psi_{water} - \Psi_{leaf}}$$

(Ψ_{water}, water potential of distilled water; $\Psi_{water} = 0$ was used in the present study).

The method of 'cutting minor veins' was widely used for estimating K_x in dicotyledonous leaves (Scoffoni & Sack, 2015). This is because in dicotyledons the bulk of water in major veins influx into minor veins and, thus, the major and minor veins act approximately in series. However, veins are parallel distributed in grass leaves, and the major and minor veins are not in series. One potential risk in K_x estimation by using the 'cutting minor veins' method in grass leaves is that water flow may mainly follow the large vessels in the major veins. To avoid this risk, we estimated the K_x by using an intact leaf rather than the middle part of the leaf (Wei *et al.*, 1999; Stiller *et al.*, 2003, 2005; Maherali *et al.*, 2008). In fact, our results showed that the size of the major vein decreases significantly from leaf base to tip in rice and that the size of veins at leaf tips tend to be uniform (similar to minor veins) (Supporting Information Fig. S1). This kind of cut is very similar with the K_x estimation method that is used widely in dicotyledonous species (Buckley *et al.*, 2015; Scoffoni & Sack, 2015). Moreover, a good correlation was obtained between measured K_x and modeled K_x ($K_{x\text{-Model}}$) (Fig. 1). In this study, K_x was measured using the method originally described by Stiller *et al.* (2003). The leaf with 2–3 cm leaf sheath was cut from the tiller underwater to avoid introducing embolism, and the apical 2–4 cm of the leaf blade was removed. Such leaf segments usually lacked continuous aerenchyma. In a similar way used in K_{leaf} measurement, the leaf sheath was contacted to the tubing system that was connected to a water-filled plastic erlenmeyer flask that could be lowered *c.* 60 cm to create pressure gradient. The leaf tip was submerged in a small water-filled cup that was placed on an electronic balance. Five different pressures (i.e. different heights) were used to measure the flow rates of water off the balance and calculated K_x from the linear regression between flow rate and applied pressure. After the measurements, the leaves were flushed at *c.* 100 kPa with water to examine the continuous aerenchyma, with the apical end submerged under the water. If large air bubbles emerged from the cut surface during the flushing, the leaf was discarded. The genotypes of Lat and Rhi were removed from the K_x analysis, because the flushing measurements indicated that they have continuous aerenchyma in all the measured leaves.

In the present study, the modeled xylem hydraulic conductance ($K_{x\text{-Model}}$, mmol m^{-2} s^{-1} MPa^{-1}) was calculated using the Hagen–Poiseuille equation (North *et al.*, 2013):

$$K_{x-Model} = \frac{\pi(h^2 \times b^2)}{128\eta} \times n \times VLA_{minor} + \frac{\pi(A^2 \times B^2)}{128\eta} \times n \times VLA_{major}$$

(h and H, height of conduit in minor and major veins (including midrib and large veins), respectively (for their determination see 'Light microscopy analysis'); b and B, width of conduit in minor and major veins, respectively; n, number of conduits per minor or major vein (sum of midrib and large veins); η, viscosity of water (8.324×10^{-10} MPa s at 28°C)). We note that this measurement may underestimate the real conductance, because the transverse veins were ignored. K_{ox} was calculated as follows:

$$\frac{1}{K_{leaf}} = \frac{1}{K_{ox}} + \frac{1}{K_x}$$

The K_{ox} was also simulated by using a model based on leaky cable theory as developed for roots (Landsberg & Fowkes, 1978) and modified for leaves (North *et al.*, 2013). In this model, the axial flow along the leaf blade declines with distance from the bases to tips along the leaf blade, and the decline is equal to radial (lateral) flow into the mesophyll. This leads to a second-order ordinary differential equation for water potential with respect to distance along the blade, with the boundary conditions that axial flow is zero at the end of the leaf, and that water potential is zero

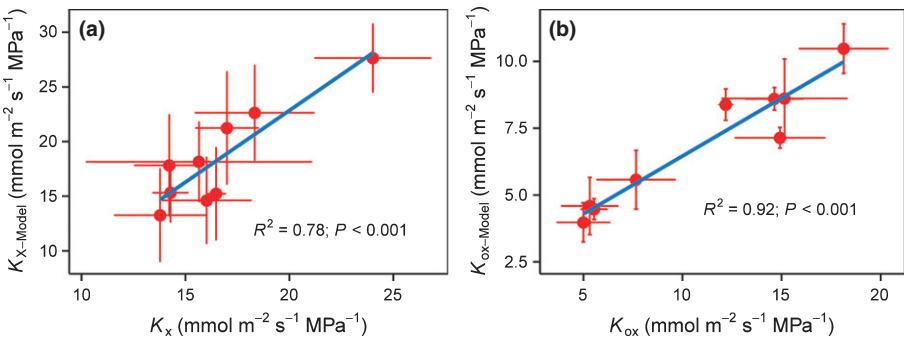

Fig. 1 The correlation between (a) measured leaf hydraulic conductance inside xylem (K_x) and modeled leaf hydraulic conductance inside xylem ($K_{x\text{-Model}}$) and (b) measured leaf hydraulic conductance outside xylem (K_{ox}) and modeled leaf hydraulic conductance outside xylem ($K_{ox\text{-Model}}$) in *Oryza*. Values are mean ± SD (n = 3–9 plants). The fitting lines are shown when P < 0.05.

at the base of the leaf. The solution can be expressed as the following relationship between K_{leaf} and K_{ox}:

$$K_{ox} = \alpha l K_{leaf}\left(\frac{\exp(2\alpha l)+1}{\exp(2\alpha l)-1}\right)$$

(l, leaf length). α is defined as:

$$\alpha = \sqrt{w\frac{K_{ox}}{K_x}}$$

(w, leaf width). Both sides of the first equation above depend on K_{ox}, but the equation cannot be solved analytically for K_{ox}; we therefore used SOLVER in Microsoft EXCEL to determine the value of K_{ox} that satisfies the equation. Then the modeled K_{ox} ($K_{ox\text{-}Model}$) was solved by input leaf width (w), leaf length (l), the modeled K_x ($K_{x\text{-}Model}$) and K_{leaf}. Because K_x and K_{ox} from measured and modeled methods were quite similar (Fig. 1), the measured K_x and K_{ox} were used to estimate the correlations with other traits.

Leaf vein length per leaf area

Leaves were cleaned in 20% aqueous NaOH after their widths were recorded and then three sections of each leaf (*c.* 5.0 mm length) were excised from the middle portion, stained with safranin O and fast green (Sigma-Aldrich), and mounted in glycerol for the determination of vein number. Rice vascular bundles can be categorized into three types based on their size: midrib, large veins and minor veins (Scarpella *et al.*, 2003; Smillie *et al.*, 2012; Xiong *et al.*, 2015d). In the present study, the numbers of major veins (sum of midrib and large veins) and minor veins were recorded using a microscope at ×40 magnification.

Light microscopy analysis

After gas exchange measurement, small leaf sections of *c.* 4.0 × 1.2 mm were also cut from the middle of new fully expanded leaves (avoiding midribs). The leaf sections were infiltrated with fixative 2.5% glutaric aldehyde in 0.1 M phosphate buffer (pH = 7.6) at 4°C with a vacuum chamber (DZF-6050; Shanghai Hasuc Co. Ltd, Shanghai, China), and post-fixed in 2% buffered osmium tetroxide at 20°C for 2 h. The samples were embedded in Spurr's epoxy resin. For light microscopy, semithin leaf cross-sections were cut using a fully automated rotary microtome (Leica RM2265; Leica Microsystems, Milton Keynes, UK). The leaf sections were stained with 1% (w/v) toluidine blue in 1% (w/v) $Na_2B_4O_7$, and they were examined at ×40 and ×100 magnification with an Olympus IX71 light microscope (Olympus Optical, Tokyo, Japan). For transmission electron microscopes (TEM), H-7650 (Hitachi – Science & Technology, Tokyo, Japan) were used for observation and photography. Three leaves in each variety or treatment were analyzed. The total cross-sectional area of mesophyll tissues (S_{mes}) and intercellular air space area (S_{IAS}), the total length of the mesophyll cell wall exposed to intercellular air space (l_m), the total length of chloroplasts touching the plasma membrane appressed to intercellular air space (l_c), and the width of the analyzed leaf cross section (L) were measured using IMAGEJ software (National Institute of Health, Bethesda, MD, USA). The volume fraction of intercellular air space (f_{IAS}) calculated as:

$$f_{IAS} = \frac{S_{IAS}}{S_{mes}}$$

S_m and S_c were then calculated as follows:

$$S = \frac{l}{L} \times F$$

where S is S_m or S_c, l is l_m or l_c, and the F is the curvature correction factor, 1.42 according to previous studies (Xiong *et al.*, 2015b). The height (a and A) and width (b and B) of conduit in at least 15 major and minor veins were measured per genotype in the light microscopy images (×40) (Fig. S2).

Scanning electron microscope analysis

Five small leaf discs (*c.* 10 × 10 mm) were removed from the middle of each leaf sections (the same leaf used for anatomy analysis) (Xiong *et al.*, 2015c). For each genotype, three leaves from different plants were measured. The leaf discs were infiltrated in a vacuum chamber (DZF-6050; Shanghai Hasuc Co. Ltd) with the fixative 2.5% glutaric aldehyde in 0.1 M phosphate buffer (pH = 7.6) at 4°C and then the samples were stored at 4°C until analysis. Six to 12 images of the abaxial and adaxial epidermal surfaces for each leaf were captured under vacuum with a scanning electron microscopes (JSM-6390LV, Tokyo, Japan). Stomatal number per measured area (stomatal density, SD), guard cell length (GL), width of entire stoma at center of the stoma (SW), stoma pore length (PL), pore width at center of the stoma (PW) and the guard cell width (GW) at the center of the stoma on the abaxial and adaxial lamina surface were measured using Image J software (National Institute of Health). In this study, the stomatal size was calculated based on the assumption that stoma is an ellipse with its major axis equal to GW and its minor axis equal to SW. More detail about the stomatal features measurement is provided in the legend for Fig. S3.

Calculating anatomical theoretical stomatal conductance

Maximum theoretical stomatal conductance to CO_2 as defined by stomatal anatomy (g_{smax}, mol m^{-2} s^{-1}) was estimated for each genotype using a double end-correction version of the equation by (Franks & Farquhar, 2001; Dow *et al.*, 2014):

$$g_{smax} = \frac{d \cdot \mathrm{SD} \cdot a_{max}}{1.6v\left(\mathrm{PD} + \frac{\pi}{2}\sqrt{\frac{a_{max}}{\pi}}\right)}$$

(d, diffusivity of water in air (24.9×10^{-6} m^{-2} s^{-1}, at 25°C); a_{max}, mean maximum stomatal pore area, defined as an ellipse with major axis equal to PL and minor axis equal to PW; v, molar

volume of air (22.4×10^{-3} m^3 mol^{-1}, at 25°C, 101.3 kPa); PD, stomatal pore depth, which is equal to GW; π, mathematical constant). The g_{smax} for each leaf was calculated as the sum of g_{smax} abaxial and adaxial. In the present study, PD and a_{max} values were genotype averages.

Statistical analysis

One-way ANOVA was used to test the differences in measured traits (Tables 1, 2) among genotypes. Regression analyses were performed with mean values to test the correlations between parameters. All regressions were fitted by both linear and power models, and the model with higher regression coefficient was selected. Regression lines was shown for $P < 0.05$. All analyses were performed in R v.3.2.2 (https://cran.r-project.org).

Results

Variation of gas exchange and K_{leaf} across genotypes

The *Oryza* genotypes used in the present study exhibited a substantial variation in photosynthetic physiology as well as leaf hydraulic physiology (Table 1). A very large range of A extending from 17.6 μmol m^{-2} s^{-1} in the Wcr to 35.9 μmol m^{-2} s^{-1} in the Lat was observed. Genotypes varied 3.1-fold in g_s, from 0.19 mol m^{-2} s^{-1} in the Rhi to 0.58 mol m^{-2} s^{-1} in the Lat. The g_m varied 4.7-fold across genotypes, from 0.10 mol m^{-2} s^{-1} in the Wcr to 0.47 in the Lat. The K_{leaf} varied from 3.31 mmol m^{-2} s^{-1} MPa^{-1} in the Rhi to 12.2 mmol m^{-2} s^{-1} MPa^{-1} in the Lat. Genotypes also differed significantly in K_x and K_{ox}. The K_x varied from 13.8 mmol m^{-2} s^{-1} MPa^{-1} in Nipponbare to 24.0 mmol m^{-2} s^{-1} MPa^{-1} in the Wcr, K_{ox} (inferred as $1/(1/K_{leaf} - 1/K_x)$) varied from 5.0 mmol m^{-2} s^{-1} MPa^{-1} in the I80 to 18.1 mmol m^{-2} s^{-1} MPa^{-1} in Huanghuazhan, the modeled K_x ($K_{x\text{-Model}}$) varied from 13.3 mmol m^{-2} s^{-1} MPa^{-1} in the Nipponbare to 29.2 mmol m^{-2} s^{-1} MPa^{-1} in Lat, and the modeled K_{ox} ($K_{ox\text{-Model}}$) varied from 3.97 mmol m^{-2} s^{-1} MPa^{-1} in the I90 to 15.2 mmol m^{-2} s^{-1} MPa^{-1} in Lat.

Leaf venation and stomatal features on K_{leaf}

In order to determine whether the K_x can be predicted from leaf vein features, the relationship between K_x and $K_{x\text{-Model}}$ was investigated. A linear relationship between K_x and $K_{x\text{-Model}}$ was observed ($R^2 = 0.78$, $P < 0.001$; $n = 3$–9; Fig. 1a). Likewise, there was a tight correlation between K_{ox} and $K_{ox\text{-Model}}$ ($R^2 = 0.92$, $P < 0.001$; Fig. 1b). Across the selected genotypes, the percentage of leaf hydraulic resistance inside xylem ($R_x/R_{leaf} = K_{leaf}/K_x$) and outside xylem ($R_{ox}/R_{leaf} = K_{leaf}/K_{ox}$) varied widely (Fig. 2). Across genotypes VLA showed a large variation, and a highly significant linear relationship was observed between K_x and VLA ($R^2 = 0.77$, $P < 0.001$). However, there was no significant positive relationship between K_{ox} and VLA ($R^2 = 0.27$, $P = 0.151$; Fig. 3). The relationships between leaf hydraulic traits and g_s are shown in Fig. S4. An earlier study found that K_{leaf} was linearly correlated with g_s across the selected genotypes ($R^2 = 0.57$, $P = 0.007$; Xiong *et al.*, 2015c), but the present study found no relationship between g_s and either K_x or K_{ox} individually (Fig. S4). Moreover, no coordination between K_x and g_{smax} nor between K_{ox} and g_{smax} was found across the selected genotypes. Stomatal density and size varied considerably among genotypes in the present study (Figs 4, S5, S6). A negative correlation between stomatal density and stomatal size was observed (Fig. 4). However, neither g_s nor K_{leaf} was correlated with stomatal density and stomatal length when data were pooled across all genotypes (Figs S5, S6).

Correlations of K_{ox}, g_m and leaf structural features

Across all genotypes, K_{ox} was linearly correlated with g_m ($R^2 = 0.70$, $P < 0.005$; Fig. 5). To explore a potential structural basis for this correlation, we investigated leaf anatomy and

Table 2 Mean values ± SD of fraction of leaf mesophyll volume occupied by intercellular air space (f_{IAS}), mesophyll cell wall thickness ($T_{cell\text{-}wall}$), mesophyll cell surface area exposed to intercellular air space per leaf area (S_m) and mesophyll cell surface area occupied by chloroplasts exposed to intercellular air space per leaf area (S_c) ($n = 3$–9 plants)

Genotype	Species	f_{IAS} (%)	$T_{cell\ wall}$ (μm)	S_m (μm² μm⁻²)	S_c (μm² μm⁻²)
Shanyou 63	*Oryza sativa* L.	19.6 ± 2.9	0.157 ± 0.009	17.9 ± 1.3	17.4 ± 2.3
Huanghuazhan	*Oryza sativa* L.	21.7 ± 2.9	0.164 ± 0.014	20.8 ± 2.0	19.6 ± 0.9
N22	*Oryza sativa* L.	18.3 ± 0.9	0.180 ± 0.003	16.8 ± 2.3	12.1 ± 2.5
Nipponbare	*Oryza sativa* L.	21.2 ± 3.1	0.165 ± 0.019	20.3 ± 2.5	17.9 ± 4.5
Lat	*Oryza latifolia* L.	23.4 ± 3.0	0.142 ± 0.017	25.4 ± 2.0	23.4 ± 2.0
Aus	*Oryza australiansis* L.	16.5 ± 1.5	0.183 ± 0.004	14.1 ± 1.3	10.7 ± 1.7
I90	*Oryza rufipogon* L.	19.9 ± 0.2	0.168 ± 0.009	18.3 ± 1.8	16.4 ± 3.2
I08	*Oryza punctata* L.	14.9 ± 1.7	0.187 ± 0.015	9.6 ± 1.8	6.6 ± 0.7
Wcr	*Oryza granulata* L.	16.3 ± 1.2	0.185 ± 0.016	11.3 ± 0.3	6.4 ± 0.7
Ruf	*Oryza rufipogon* L.	17.2 ± 2.2	0.180 ± 0.014	12.6 ± 1.7	9.2 ± 5.9
Rhi	*Oryza rufipogon* L.	16.5 ± 1.7	0.154 ± 0.023	16.1 ± 1.8	15.0 ± 1.6
ANOVA					
Average		18.7 ± 2.6	0.169 ± 0.015	16.7 ± 4.6	14.1 ± 5.5
Genotype		*	*	**	***

*, $P < 0.05$; **, $P < 0.01$; ***, $P < 0.001$.

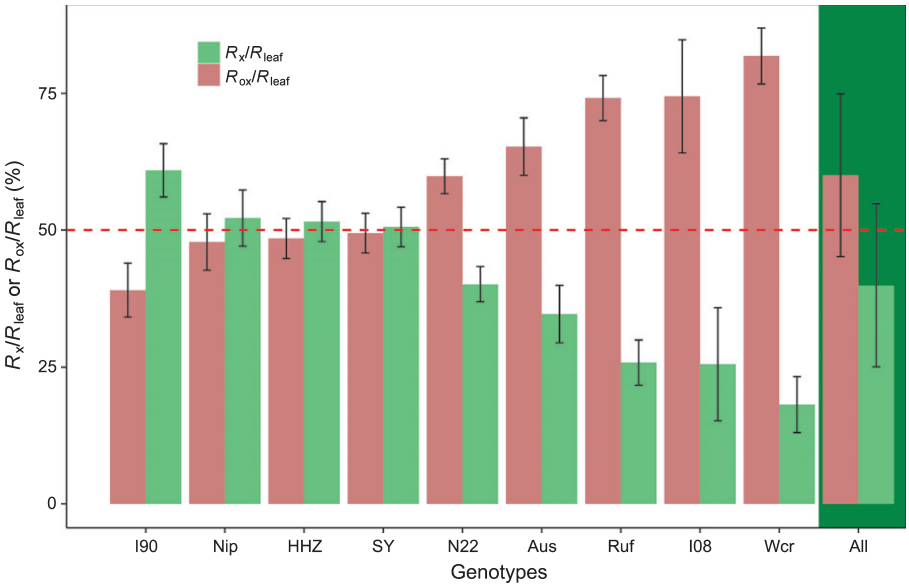

Fig. 2 The percentage of leaf hydraulic resistance inside xylem (resistance of the leaf xylem (R_x)/resistance of the leaf (R_{leaf})) and leaf hydraulic resistance outside xylem (resistance of the leaf xylem (R_{ox})/resistance of the leaf (R_{leaf})) in *Oryza*. Values are mean ± SD (n = 3–9 plants).

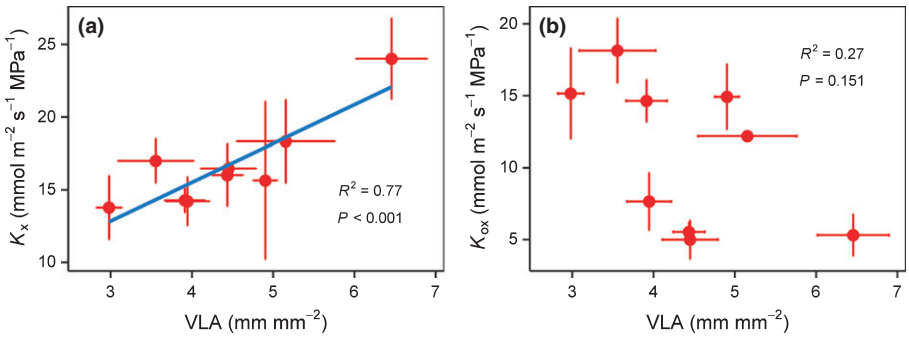

Fig. 3 The correlation between (a) leaf hydraulic conductance inside xylem (K_x) and leaf vein length per leaf area (VLA) and (b) leaf hydraulic conductance outside xylem (K_{ox}) and VLA in *Oryza*. Values are mean ± SD (n = 3–9 plants). The fitting lines are shown when P < 0.05.

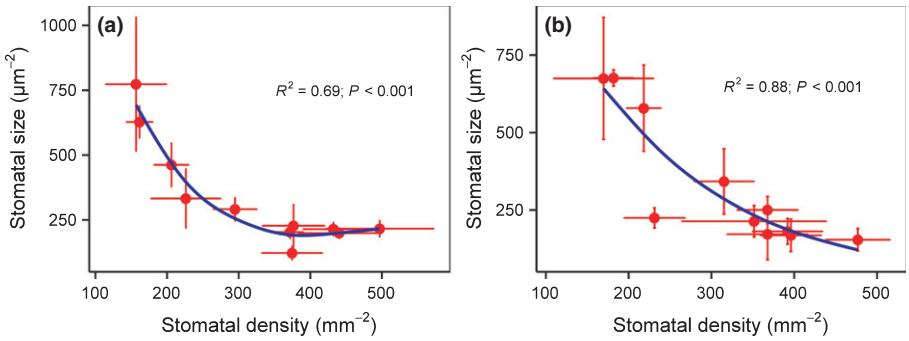

Fig. 4 Correlations between the stomatal density and stomatal size at (a) abaxial side and (b) adaxial side across *Oryza* genotypes. Values are mean ± SD (n = 3–9 plants).

structure features. For all examined anatomical traits, there were very large differences among genotypes. Across all genotypes, fraction of leaf mesophyll volume occupied by intercellular air space (f_{IAS}) varied from 15% to 23% and mesophyll cell wall thickness (T_{cw}) varied from 0.142 to 0.187 μm (Table 2). Genotypes varied by 2.6-fold in mesophyll cell surface area exposed to intercellular air space per leaf area (S_m) and 3.7-fold in chloroplast cell surface area exposed to intercellular air space per leaf area (S_c). Across all genotypes, g_m increased with f_{IAS} (R^2 = 0.56, P < 0.01), S_m (R^2 = 0.82, P < 0.001) and S_c (R^2 = 0.77, P < 0.001); however, g_m decreased with T_{cw} (R^2 = 0.80, P < 0.001) across all genotypes. Similar correlations were observed between K_{ox} and leaf anatomical traits (Fig. 6).

Discussion

Water transport and CO_2 diffusion inside leaves are two important functional traits that determine the CO_2 assimilation efficiency (Sack & Holbrook, 2006; Flexas *et al.*, 2013b). In our previous study (Xiong *et al.*, 2015c), we found that both leaf

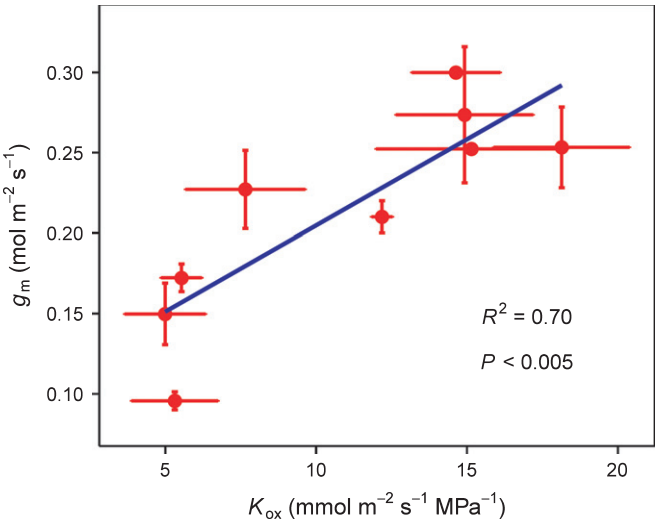

Fig. 5 Relationship between mesophyll conductance to CO_2 (g_m) and leaf hydraulic conductance outside xylem (K_{ox}) in *Oryza*. Values are mean ± SD (n = 3–9 plants).

hydraulic conductance (K_{leaf}) and mesophyll conductance (g_m) varied widely among *Oryza* genotypes, and showed a large degree of correlation with one another. In the current study, our detailed examination of leaf functional and anatomical features provides new insight into the variation of K_{leaf} and g_m across related genotypes and their correlations.

Partitioning leaf hydraulic resistance ($R_{leaf} = 1/K_{leaf}$) into xylem and outside-xylem components is a key step to understanding leaf hydraulic design. Our results presented here show that the percentage of outside xylem hydraulic resistance varied from 39.1% to 81.8%, and averaged *c.* 60% in rice and rice relatives leaves (Table 1), implying that outside-xylem pathways exert slightly more control over K_{leaf} than xylem pathways, on average across genotypes. This finding is consistent with previous studies on partitioning hydraulic resistances inside leaves which showed that hydraulic resistances within the xylem are on the same order as those outside of the xylem and vary significantly across species (Sack *et al.*, 2004, 2005; Nardini *et al.*, 2005, 2010). For instance, Sack *et al.* (2005) found that percentage of outside xylem hydraulic resistance varied from 11% to 74% across 10 tropical rainforest tree species. The variation of partitioning leaf hydraulic resistance across genotypes may relate to leaf anatomy.

The correlations between K_{leaf} and leaf vein traits have been widely studied and the best supported vein anatomical correlate of K_{leaf} is vein length per area (VLA; Caringella *et al.*, 2015). In the present study, we found that leaf hydraulic conductance inside xylem (K_x) was linearly correlated with VLA, but no correlation was found between leaf hydraulic conductance outside xylem (K_{ox}) and VLA. This finding indicates that VLA mainly impacts K_x rather than K_{ox} (Cochard *et al.*, 2004). Moreover, a tight relationship between K_x and modeled K_x ($K_{x\text{-Model}}$), which is calculated from vein anatomical traits from Poiseuille's Law, indicates that K_x is related to leaf vein anatomy. Several previous studies observed that the species with high VLA tends to increase K_{ox} due to the shorter water transport pathway from veins to stoma (Sack & Frole, 2006; Brodribb *et al.*, 2007; Buckley *et al.*, 2015). In the rice leaves the stoma clustered around leaf veins (Fig. S7), which indicates that although the distance between veins varied across genotypes the water transport pathways are relatively consistent. K_{leaf} but also anatomical traits like stomatal density and size are often shown to determine stomatal conductance (g_s) (Ocheltree *et al.*, 2012). However, in the present study, stomatal anatomical traits showed no relationship with g_s across *Oryza* genotypes (Fig. S5), contrary to previous reports suggesting that differences of g_s across genotypes are related to the variation of stomatal anatomical traits under drought conditions (Xu & Zhou, 2008). Although a wide variation of stomatal size and density were found across the selected genotypes, the g_{smax} value calculated from stomatal anatomy showed a narrow variation across genotypes (from 0.83 to 1.07 mol m^{-2} s^{-1}). Our result suggests that *Oryza* genotypes used in this study have a similar potential maximum g_s and that the differences of g_s between genotypes might be determined by regulatory mechanisms and/or leaf water status. Indeed, g_s was found to be significantly correlated to K_{leaf} (Xiong *et al.*, 2015d) but not to either of its two components, K_x or K_{ox} (Fig. S4).

In summary, across the selected *Oryza* genotypes, g_s is mostly dependent on K_{leaf} but not on stomatal features that determine maximum theoretical g_s, and K_{leaf} in turn is limited more by K_{ox} than by K_x, although the contributions of K_x and K_{ox} varied widely across genotypes (Cochard *et al.*, 2004; North *et al.*, 2013). In addition, the relationship between g_s and g_m pooling all genotypes, although significant, was relatively scattered. The ratio g_m/g_s, which is important in leaf water-use efficiency (Flexas *et al.*, 2013a; Buckley & Warren, 2014), was highly variable, ranging from 0.48 in Wcr to 1.47 in Rhi. Altogether, these characteristics make this collection of *Oryza* genotypes suitable for studying the relationships between K_{leaf} and g_m without a strong interference of indirect relationships caused by the interdependency of g_s and g_m. Indeed, g_m was strongly correlated with K_{ox} (Fig. 5), whereas g_s was not (Fig. 2).

The tight relationship between g_m and K_{ox} suggested that water and CO_2 share a significant fraction of their respective flow pathways inside leaves, so they are also expected to share some anatomical determinants – mostly likely involving the mesophyll and intercellular air spaces (Flexas *et al.*, 2013a,b). In the present study, across all genotypes, K_{ox} increased with volume fraction of intercellular air space (f_{IAS}) (Fig. 6b).This is consistent with simulations by Buckley *et al.* (2015), who attributed the role of f_{IAS} to the contribution of vapor transport to K_{ox}. The possibility that vapor diffusion may contribute substantially to water transport within leaf was also suggested by Rockwell *et al.* (2014) and Buckley (2015). This suggests that gas-phase transport may play an important role in outside-xylem water transport and that the liquid water evaporates deep within the leaf and/or along the transport pathway. In this study, g_m also was correlated with f_{IAS}, contrary to observations in nongrass species (Tomás *et al.*, 2013). f_{IAS} can affect g_m in two ways: by increasing gas-phase CO_2 diffusion, and by increasing the number of parallel diffusion pathways from outer surfaces of cell walls to chloroplasts (intercellular air

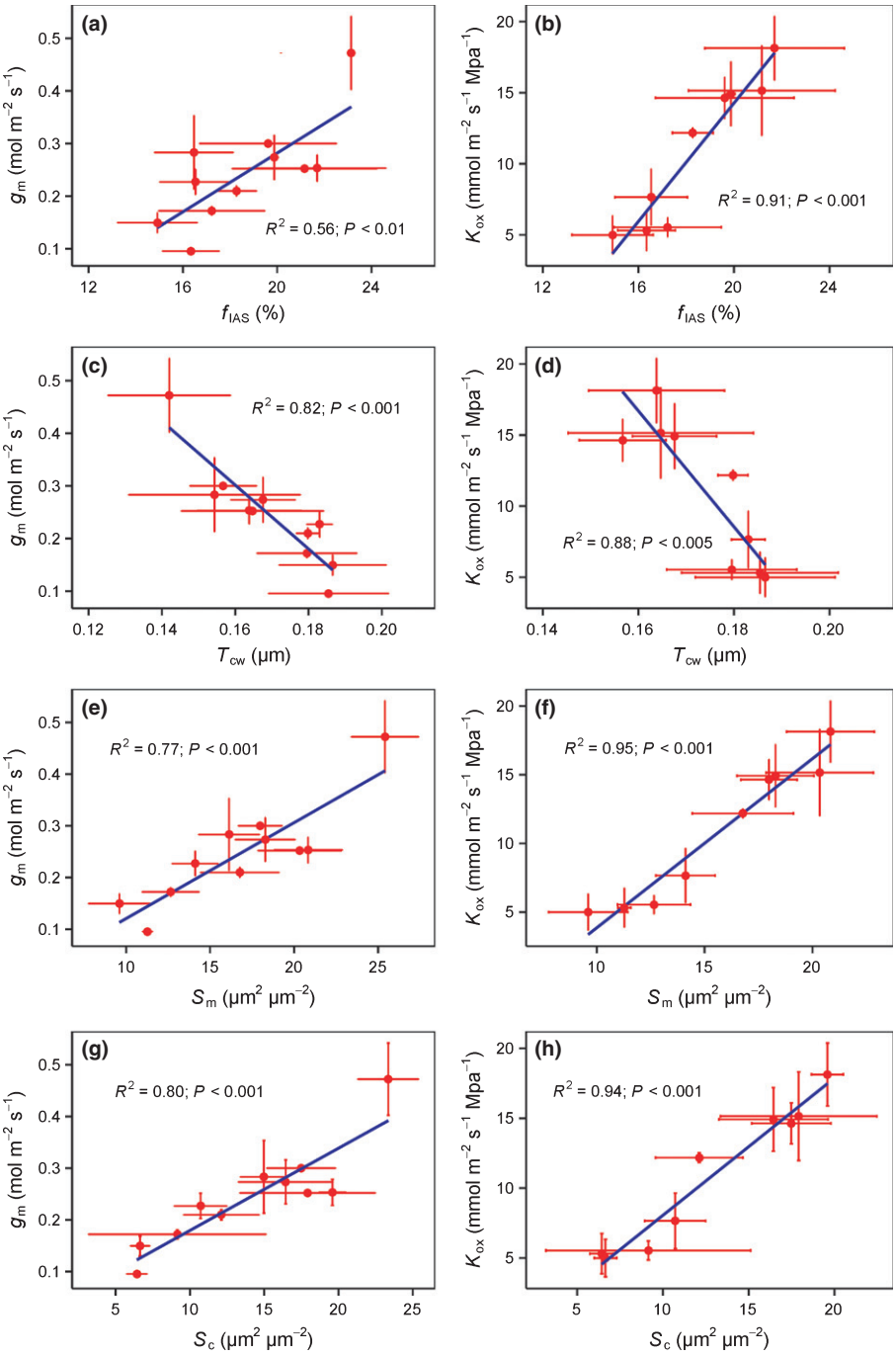

Fig. 6 Effects of (a, b) fraction of leaf mesophyll volume occupied by intercellular air space (f_{IAS}), (c, d) mesophyll cell wall thickness ($T_{cell\text{-}wall}$), (e, f) mesophyll cell surface area exposed to intercellular air space per leaf area (S_m) and (g, h) mesophyll cell surface area occupied by chloroplasts exposed to intercellular air space per leaf area (S_c) on mesophyll conductance to CO_2 (g_m) and leaf hydraulic conductance (K_{leaf}) in *Oryza*. Values are mean ± SD (n = 3–9 plants).

space per unit leaf area (S_m) and mesophyll cell surface area occupied by chloroplasts exposed to intercellular air space per leaf area (S_c)). Although it is likely that gaseous diffusion plays a role in g_m variation across genotypes, it is not the major factor because the diffusion of CO_2 in the gaseous phase is 10^4 times faster than that in the liquid phase (Evans *et al.*, 2009). Thus, the tight correlation between f_{IAS} and g_m would be by increasing parallel diffusion pathways, which was also supported by the correlation between f_{IAS} and S_m (Fig. S8).

The apoplastic transport pathway, which should be closely related to cell wall thickness, has been suggested as the major water transport pathway outside xylem. For instance, Buckley *et al.* (2015) found that K_{ox} was increased by 370% when cell wall thicknesses used in simulations were increased five-fold. By contrast, we found that K_{ox} decreased with cell wall thickness across the selected *Oryza* genotypes. However, in the present study, the cell wall thickness only ranged from 0.15 to 0.19 µm across genotypes, whereas K_{ox} varied over three-fold across the same range, which suggests that the observed negative correlation between cell wall thickness and K_{leaf} might be due to the influence of other traits. For example, cell wall thickness significantly decreased with increasing nitrogen (N) supplements in rice

(Xiong *et al.*, 2015b), yet K_{leaf} is positively correlated with leaf N content (Xiong *et al.*, 2015d).

Our results showed that both g_m and K_{ox} increased linearly with S_m across genotypes. The relationship of S_m/S to g_m has been discussed previously (e.g. Flexas *et al.*, 2012) and may reflect the quantity of CO_2-transporting membrane proteins, which should scale with membrane area and thus cell surface area. The relationship of S_m to K_{ox} is novel, however, and merits further discussion. According to Farquhar & Raschke (1978), the liquid water evaporates at the mesophyll surface along transport pathway. K_{ox} is defined as the ratio of water flow rate through the living tissues of the leaf to the driving force (i.e. the water potential difference between leaf vein and evaporating sites), so an increase in the evaporating surface area, S_m, will increase K_{ox}. In the present study, we also found a tight relationship between K_{ox} and S_c, but this correlation may arise due to the covariation of S_m and S_c in rice (Fig. S8). In fact, under normal conditions almost all of the cell surface is occupied by chloroplasts (Sage & Sage, 2009; Xiong *et al.*, 2015a; also see Fig. S9). Our results suggested that S_m might be one of the key mesophyll anatomical trait mediating the correlation of g_m and K_{ox} in rice.

A recent modeling and empirical study suggested that the dominant water transport resistance outside the xylem occurs in the spongy mesophyll (Buckley *et al.*, 2015) due to the low cell-to-cell connectivity. Here, we estimated the spongy mesophyll structural traits that may contribute to both K_{ox} and g_m in *Oryza*, and found that f_{IAS} and S_m play an important role in K_{ox}. However, despite the strong correlations found, we cannot conclude that K_{ox} is limited only by the mesophyll structural traits investigated here. In fact, mesophyll structural traits are often correlated with each other, for example, mesophyll cell thickness is correlated with cell size and mesophyll thickness across species (John *et al.*, 2013). The role of leaf anatomical traits in determining K_{ox} (then K_{leaf}) remains an important focus for future work.

In conclusion, this study presents the first evidence of a strong correlation between K_{ox} and g_m, mediated by variation in mesophyll traits across rice genotypes. Our data also showed that outside-xylem contributed *c.* 60% of leaf hydraulic resistance, although this percentage varied strongly among genotypes. Furthermore, we found that both K_{leaf} and g_s were independent of stomatal density or size. A detailed understanding of the coordination of leaf anatomy, carbon assimilation and water transportation can provide a clearer ability to scale up from physiological processes to whole leaf function. Further research is needed to understand the developmental basis for this coordination, specially, under dynamic environmental conditions.

Acknowledgements

This work was supported by Major International Joint Research Project of NSFC (no. 31361140368) and the Program for Changjiang Scholars and Innovative Research Team in University of China (IRT1247). Jaume Flexas acknowledges funding from Plan Nacional, Spain (contracts BFU2011-23294 and CTM2014-53902-C2-1-P). The authors thank Dr Thomas N. Buckley for expert assistance in developing the leaky cable model and his valuable comments on the manuscript, Dr Cyril Douthe for his useful comments for the study, and three anonymous reviewers for their constructive criticism of the manuscript. D.X. thanks the China Scholarship Council (CSC) for the funding of joint training PhD.

Author contributions

D.X. planned and designed the research; D.X. and T.Y. performed the experiments; D.X. and J.F. analyzed the data; D.X., J.F., J.H. and S.P. wrote the manuscript.

References

Bernacchi CJ, Portis AR, Nakano H, von Caemmerer S, Long SP. 2002. Temperature response of mesophyll conductance. Implications for the determination of Rubisco enzyme kinetics and for limitations to photosynthesis *in vivo*. *Plant Physiology* **130**: 1992–1998.

Blonder B, Violle C, Bentley LP, Enquist BJ. 2011. Venation networks and the origin of the leaf economics spectrum. *Ecology Letters* **14**: 91–100.

Brodribb TJ, Feild TS, Jordan GJ. 2007. Leaf maximum photosynthetic rate and venation are linked by hydraulics. *Plant Physiology* **144**: 1890–1898.

Brodribb TJ, Holbrook NM. 2004. Stomatal protection against hydraulic failure: a comparison of coexisting ferns and angiosperms. *New Phytologist* **162**: 663–670.

Brodribb TJ, McAdam SAM. 2011. Passive origins of stomatal control in vascular plants. *Science* **331**: 582–585.

Buckley TN. 2015. The contributions of apoplastic, symplastic and gas phase pathways for water transport outside the bundle sheath in leaves. *Plant, Cell & Environment* **38**: 7–22.

Buckley TN, John GP, Scoffoni C, Sack L. 2015. How does leaf anatomy influence water transport outside the xylem? *Plant Physiology* **168**: 1616–1635.

Buckley TN, Warren CR. 2014. The role of mesophyll conductance in the economics of nitrogen and water use in photosynthesis. *Photosynthesis Research* **119**: 77–88.

Caringella MA, Bongers FJ, Sack L. 2015. Leaf hydraulic conductance varies with vein anatomy across *Arabidopsis thaliana* wild-type and leaf vein mutants. *Plant, Cell & Environment* **38**: 2735–2746.

Cochard H, Nardini A, Coll L. 2004. Hydraulic architecture of leaf blades: where is the main resistance? *Plant, Cell & Environment* **27**: 1257–1267.

Dow GJ, Berry JA, Bergmann DC. 2014. The physiological importance of developmental mechanisms that enforce proper stomatal spacing in *Arabidopsis thaliana*. *New Phytologist* **201**: 1205–1217.

Ethier GJ, Livingston NJ. 2004. On the need to incorporate sensitivity to CO_2 transfer conductance into the Farquhar–von Caemmerer-Berry leaf photosynthesis model. *Plant, Cell and Environment* **27**: 137–153.

Evans JR, Kaldenhoff R, Genty B, Terashima I. 2009. Resistances along the CO_2 diffusion pathway inside leaves. *Journal of Experimental Botany* **60**: 2235–2248.

Farquhar GD, Raschke K. 1978. On the resistance to transpiration of the sites of evaporation within the leaf. *Plant Physiology* **61**: 1000–1005.

Flexas J, Barbour MM, Brendel O, Cabrera HM, Carriquí M, Díaz-Espejo A, Douthe C, Dreyer E, Ferrio JP, Gago J *et al.* 2012. Mesophyll diffusion conductance to CO_2: an unappreciated central player in photosynthesis. *Plant Science* **193–194**: 70–84.

Flexas J, Niinemets Ü, Gallé A, Barbour M, Centritto M, Diaz-Espejo A, Douthe C, Galmés J, Ribas-Carbo M, Rodriguez P *et al.* 2013a. Diffusional conductances to CO_2 as a target for increasing photosynthesis and photosynthetic water-use efficiency. *Photosynthesis Research* **117**: 45–59.

Flexas J, Ribas-Carbo M, Diaz-Espejo A, Galmes J, Medrano H. 2008. Mesophyll conductance to CO_2: current knowledge and future prospects. *Plant, Cell & Environment* **31**: 602–621.

Flexas J, Scoffoni C, Gago J, Sack L. 2013b. Leaf mesophyll conductance and leaf hydraulic conductance: an introduction to their measurement and coordination. *Journal of Experimental Botany* **64**: 3965–3981.

Franks PJ, Farquhar GD. 2001. The effect of exogenous abscisic acid on stomatal development, stomatal mechanics, and leaf gas exchange in *Tradescantia virginiana*. *Plant Physiology* **125**: 935–942.

Giuliani R, Koteyeva N, Voznesenskaya E, Evans MA, Cousins AB, Edwards GE. 2013. Coordination of leaf photosynthesis, transpiration, and structural traits in rice and wild relatives (*Genus Oryza*). *Plant Physiology* **162**: 1632–1651.

Guyot G, Scoffoni C, Sack L. 2012. Combined impacts of irradiance and dehydration on leaf hydraulic conductance: insights into vulnerability and stomatal control. *Plant, Cell & Environment* **35**: 857–871.

Harley PC, Loreto F, Di Marco G, Sharkey TD. 1992. Theoretical considerations when estimating the mesophyll conductance to CO_2 flux by analysis of the response of photosynthesis to CO_2. *Plant Physiology* **98**: 1429–1436.

John GP, Scoffoni C, Sack L. 2013. Allometry of cells and tissues within leaves. *American Journal of Botany* **100**: 1936–1948.

Landsberg J, Fowkes N. 1978. Water movement through plant roots. *Annals of Botany* **42**: 493–508.

Maherali H, Sherrard ME, Clifford MH, Latta RG. 2008. Leaf hydraulic conductivity and photosynthesis are genetically correlated in an annual grass. *New Phytologist* **180**: 240–247.

McAdam SA, Brodribb TJ. 2013. Ancestral stomatal control results in a canalization of fern and lycophyte adaptation to drought. *New Phytologist* **198**: 429–441.

Nardini A, Gortan E, Salleo S. 2005. Hydraulic efficiency of the leaf venation system in sun- and shade-adapted species. *Functional Plant Biology* **32**: 953–961.

Nardini A, Pedà G, Rocca NL. 2012. Trade-offs between leaf hydraulic capacity and drought vulnerability: morpho-anatomical bases, carbon costs and ecological consequences. *New Phytologist* **196**: 788–798.

Nardini A, Qunapuu-Pikas E, Savi T. 2014. When smaller is better: leaf hydraulic conductance and drought vulnerability correlate to leaf size and venation density across four *Coffea arabica* genotypes. *Functional Plant Biology* **41**: 972–982.

Nardini A, Raimondo F, Lo Gullo MA, Salleo S. 2010. Leafminers help us understand leaf hydraulic design. *Plant, Cell & Environment* **33**: 1091–1100.

North GB, Lynch FH, Maharaj FDR, Phillips CA, Woodside WT. 2013. Leaf hydraulic conductance for a tank bromeliad: axial and radial pathways for moving and conserving water. *Frontiers in Plant Science* **4**: e78.

Ocheltree TW, Nippert JB, Prasad PVV. 2012. Changes in stomatal conductance along grass blades reflect changes in leaf structure. *Plant, Cell & Environment* **35**: 1040–1049.

Rockwell FE, Holbrook NM, Stroock AD. 2014. The competition between liquid and vapor transport in transpiring leaves. *Plant Physiology* **164**: 1741–1758.

Sack L, Frole K. 2006. Leaf structural diversity is related to hydraulic capacity in tropical rain forest trees. *Ecology* **87**: 483–491.

Sack L, Holbrook NM. 2006. Leaf hydraulics. *Annual Review of Plant Biology* **57**: 361–381.

Sack L, Melcher PJ, Zwieniecki MA, Holbrook NM. 2002. The hydraulic conductance of the angiosperm leaf lamina: a comparison of three measurement methods. *Journal of Experimental Botany* **53**: 2177–2184.

Sack L, Scoffoni C. 2012. Measurement of leaf hydraulic conductance and stomatal conductance and their responses to irradiance and dehydration using the evaporative flux method (EFM). *Journal of Visualized Experiments* **70**: e4179.

Sack L, Scoffoni C. 2013. Leaf venation: structure, function, development, evolution, ecology and applications in the past, present and future. *New Phytologist* **198**: 983–1000.

Sack L, Scoffoni C, John GP, Poorter H, Mason CM, Mendez-Alonzo R, Donovan LA. 2013. How do leaf veins influence the worldwide leaf economic spectrum? Review and synthesis. *Journal of Experimental Botany* **64**: 4053–4080.

Sack L, Scoffoni C, Johnson DM, Buckley TN, Brodribb TJ. 2015. The anatomical determinants of leaf hydraulic function. In: Hacke U, ed. *Functional and ecological xylem anatomy*. New York, NY, USA: Springer, 255–271.

Sack L, Scoffoni C, McKown AD, Frole K, Rawls M, Havran JC, Tran H, Tran T. 2012. Developmentally based scaling of leaf venation architecture explains global ecological patterns. *Nature Communications* **3**: 837.

Sack L, Streeter CM, Holbrook NM. 2004. Hydraulic analysis of water flow through leaves of sugar maple and red oak. *Plant Physiology* **134**: 1824–1833.

Sack L, Tyree MT, Holbrook NM. 2005. Leaf hydraulic architecture correlates with regeneration irradiance in tropical rainforest trees. *New Phytologist* **167**: 403–413.

Sage TL, Sage RF. 2009. The functional anatomy of rice leaves: implications for refixation of photorespiratory CO_2 and efforts to engineer C_4 photosynthesis into rice. *Plant Cell and Physiology* **50**: 756–772.

Salleo S, Raimondo F, Trifilo P, Nardini A. 2003. Axial-to-radial water permeability of leaf major veins: a possible determinant of the impact of vein embolism on leaf hydraulics? *Plant, Cell & Environment* **26**: 1749–1758.

Scarpella E, Rueb S, Meijer AH. 2003. The *RADICLELESS1* gene is required for vascular pattern formation in rice. *Development* **130**: 645–658.

Scoffoni C. 2015. Modelling the outside-xylem hydraulic conductance: towards a new understanding of leaf water relations. *Plant, Cell & Environment* **38**: 4–6.

Scoffoni C, Sack L. 2015. Testing for a Wheeler-type effect in leaf xylem hydraulic decline. *Plant, Cell & Environment* **38**: 534–543.

Sheriff DW, Meidner H. 1974. Water pathways in leaves of *Hedera helix* L. and *Tradescantia virginiana* L. *Journal of Experimental Botany* **25**: 1147–1156.

Smillie IRA, Pyke KA, Murchie EH. 2012. Variation in vein density and mesophyll cell architecture in a rice deletion mutant population. *Journal of Experimental Botany* **63**: 4563–4570.

Stiller V, Lafitte HR, Sperry JS. 2003. Hydraulic properties of rice and the response of gas exchange to water stress. *Plant Physiology* **132**: 1698–1706.

Stiller V, Sperry JS, Lafitte R. 2005. Embolized conduits of rice (*Oryza sativa*, Poaceae) refill despite negative xylem pressure. *American Journal of Botany* **92**: 1970–1974.

Tomás M, Flexas J, Copolovici L, Galmés J, Hallik L, Medrano H, Ribas-Carbó M, Tosens T, Vislap V, Niinemets Ü. 2013. Importance of leaf anatomy in determining mesophyll diffusion conductance to CO_2 across species: quantitative limitations and scaling up by models. *Journal of Experimental Botany* **64**: 2269–2281.

Ueno O, Kawano Y, Wakayama M, Takeda T. 2006. Leaf vascular systems in C_3 and C_4 grasses: a two-dimensional analysis. *Annals of Botany* **97**: 611–621.

Valentini R, Epron D, De Angelis P, Matteucci G, Dreyer E. 1995. *In situ* estimation of net CO_2 assimilation, photosynthetic electron flow and photorespiration in *Turkey oak* (*Q. cerris* L.) leaves: diurnal cycles under different levels of water supply. *Plant, Cell & Environment* **18**: 631–640.

Warren CR, Dreyer E. 2006. Temperature response of photosynthesis and internal conductance to CO_2: results from two independent approaches. *Journal of Experimental Botany* **57**: 3057–3067.

Wei C, Tyree MT, Steudle E. 1999. Direct measurement of xylem pressure in leaves of intact maize plants. A test of the cohesion-tension theory taking hydraulic architecture into consideration. *Plant Physiology* **121**: 1191–1205.

Xiong D, Chen J, Yu T, Gao W, Ling X, Li Y, Peng S, Huang J. 2015a. SPAD-based leaf nitrogen estimation is impacted by environmental factors and crop leaf characteristics. *Scientific Reports* **5**: 13 389.

Xiong D, Liu X, Liu L, Douthe C, Li Y, Peng S, Huang J. 2015b. Rapid responses of mesophyll conductance to changes of CO_2 concentration, temperature and irradiance are affected by N supplements in rice. *Plant, Cell & Environment* **38**: 2541–2550.

Xiong D, Yu T, Liu X, Li Y, Peng S, Huang J. 2015c. Heterogeneity of photosynthesis within leaves is associated with alteration of leaf structural features and leaf N content per leaf area in rice. *Functional Plant Biology* **42**: 687–696.

Xiong D, Yu T, Zhang T, Li Y, Peng S, Huang J. 2015d. Leaf hydraulic conductance is coordinated with leaf morpho-anatomical traits and

nitrogen status in the genus *Oryza*. *Journal of Experimental Botany* **66**: 741–748.

Xu Z, Zhou G. 2008. Responses of leaf stomatal density to water status and its relationship with photosynthesis in a grass. *Journal of Experimental Botany* **59**: 3317–3325.

Yin X, Struik PC, Romero P, Harbinson J, Evers JB, PE VDP, Vos J. 2009. Using combined measurements of gas exchange and chlorophyll fluorescence to estimate parameters of a biochemical C_3 photosynthesis model: a critical appraisal and a new integrated approach applied to leaves in a wheat (*Triticum aestivum*) canopy. *Plant, Cell & Environment* **32**: 448–464.

Supporting Information

Additional Supporting Information may be found online in the Supporting Information tab for this article:

Fig. S1 The vein size at the tip and at the middle of *Wcr* leaf.

Fig. S2 Diagram illustrating details of leaf anatomy (*Shanyou 63*).

Fig. S3 Diagram illustrating details of stomatal features (*Shanyou 63*).

Fig. S4 The relationships between: stomatal conductance to CO_2 (g_s) and leaf hydraulic conductance inside xylem (K_x); g_s and leaf hydraulic conductance outside xylem (K_{ox}); maximum theoretical stomatal conductance to CO_2 (g_{smax}) and K_x and (d) g_{smax} and K_{ox}.

Fig. S5 Effects of stomatal size and stomatal density of abaxial and adaxial lamina on stomatal conductance to CO_2 (g_s) across the *Oryza* genotypes.

Fig. S6 Effects of stomatal size and stomatal density of abaxial and adaxial lamina on leaf hydraulic conductance (K_{leaf}) across the *Oryza* genotypes.

Fig. S7 The distribution of stoma on adaxial lamina in two genotypes.

Fig. S8 Relationship between mesophyll cell wall surface area exposed to intercellular air space per leaf area (S_m) and fraction of leaf mesophyll volume occupied by intercellular air space (f_{IAS}) in rice.

Fig. S9 Relationship between mesophyll cell wall surface area exposed to intercellular air space per leaf area (S_m) and mesophyll cell surface area occupied by chloroplasts exposed to intercellular air space per leaf area (S_c) in rice, transmission electron microscope image of Aus and I08.

Please note: Wiley Blackwell are not responsible for the content or functionality of any Supporting Information supplied by the authors. Any queries (other than missing material) should be directed to the *New Phytologist* Central Office.